BBAA VI International Colloquium on:
Bluff Bodies Aerodynamics & Applications
Milano, Italy, July, 20–24 2008

DRAG REDUCTION OF BLUNT TRAILING-EDGE AIRFOILS

Jonathon P. Baker⋆ and C.P. van Dam⋆

⋆ Department of Mechanical and Aeronautical
University of California, Davis
Davis, CA 95616, USA
e-mails: jpbaker@ucdavis.edu, cpvandam@ucdavis.edu

Keywords: Blunt trailing edge, Airfoil, CFD, Experiment

1 INTRODUCTION

Blunt trailing-edge airfoils have been proposed to address the need for thick airfoil sections necessary to meet the structural and volume requirements of various aerodynamic systems, including blended wing-body aircraft, unmanned aerial vehicles, and wind turbine blades, while reducing the well-documented separation sensitivity of airfoils with maximum thickness-to-chord ratios greater than 25% [1, 2]. Several studies have investigated these so-called "thick" airfoils and show that blunt trailing-edge airfoils have significantly improved lift performance compared to similar sharp trailing-edge airfoils [2–7]. The use of a blunt trailing-edge, however, introduces base drag and possible vortex shedding.

Past studies have investigated several options for bluff body drag reduction [8–12], but most of this research is directed toward 2D axisymmetric bodies aligned with the flowfield [13]. Limited research has been conducted for bodies at incidence to the flow and even less study has been conducted for asymmetric lifting bodies, such as blunt trailing-edge airfoils. In the present study, the results of a coupled computational fluid dynamics (CFD) and wind tunnel experimentation study are presented for simple, static, trailing-edge attachments applied to a blunt trailing-edge airfoil in two-dimensional flow.

2 GEOMETRY

The baseline airfoil used in the present study was an FB-3500-1750 airfoil, a 35% thick variant of the FB airfoil series [14] with a 17.5% chord trailing-edge thickness, shown in Fig. 1. For the present study, simple and effective drag reduction techniques were desired. For these reasons, the drag reduction devices applied to the FB-3500-1750 in this study were limited to fixed geometric modifications to the trailing-edge, namely splitter plates, base cavities, and offset cavities, as illustrated in Fig. 2.

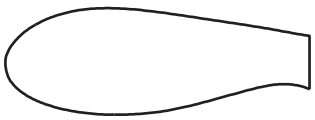

Figure 1: FB-3500-1750 Airfoil.

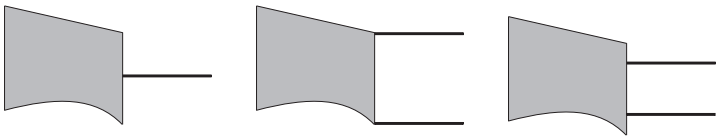

(a) (b) (c)

Figure 2: Trailing edge devices investigated include (a) simple splitter, (b) base cavity, and (c) offset cavity.

3 EXPERIMENTAL METHODS

The Aeronautical Wind Tunnel (AWT) at the University of California, Davis is an open circuit, low-turbulence wind tunnel [15]. The wind tunnel has test section area dimensions of 0.86 m $\times$ 1.22 m (2.8 ft $\times$ 4 ft) and length of 3.66 m (12 ft).

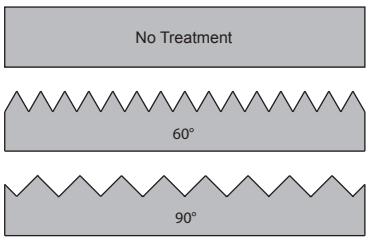

Figure 3: Edge treatments for the splitter and cavity used in experiment.

The FB-3500-1750 airfoil model was constructed with a chord length of 0.2032 m (8 in.), span of 0.8382 m (33 in.), and maximum thickness of 0.071 m (35% chord). The model was tested at a chord Reynolds number of 666,000, selected to limit solid blockage, and to avoid exceeding load limitations of the pyramidal balance. Boundary-layer transition was fixed using 0.25 mm zigzag trip-tape placed at 2% and 5% chord on the suction and pressure surfaces, respectively.

The trailing edge devices used in the experiment consist of metal plates attached perpendicular to the trailing edge of the FB-3500-1750 airfoil model, each with lengths equal to the model trailing edge thickness (17.5% chord). The device configurations investigated include the simple spltter and base cavity, shown in Fig. 2(a) and 2(b), respectively. To determine if plate edge-shape can affect device performance, three edge treatments were investigated for each device configuration including a non-serrated edge, and 90° and 60° serrated edges, as depicted in Fig. 3.

4 COMPUTATIONAL METHODS

The Reynolds-Averaged Navier–Stokes (RANS) code used in this project is OVERFLOW, a three-dimensional, compressible, structured overset grid flow solver [16]. Unsteady simulations were conducted, utilizing dual time-stepping to obtain second-order accuracy in time, with 10 to 15 subiterations per physical timestep. All meshes for the calculations in this study were generated with the Chimera Grid Tools and OVERGRID codes [17]. The simple geometries allowed for the use of O-grids, while the more complex geometries required the use of overset grid techniques.

Turbulent closure of the RANS equations is provided by the two-equation k-ω shear-stress transport (SST) model developed by Menter [18, 19]. The model is known for improved prediction of flows with strong adverse pressure gradients and separation [20], which is of particular importance in a blunt trailing-edge airfoil wake.

Most of the computational study was conducted at $Ma = 0.2$ and $Re = 666{,}000$ to closely match the reference conditions of the wind tunnel experimentation. The more promising drag reduction design configurations were also investigated at $Re = 5 \times 10^6$ in order to more closely match conditions faced by full-scale wind turbines; these cases will not be presented in this

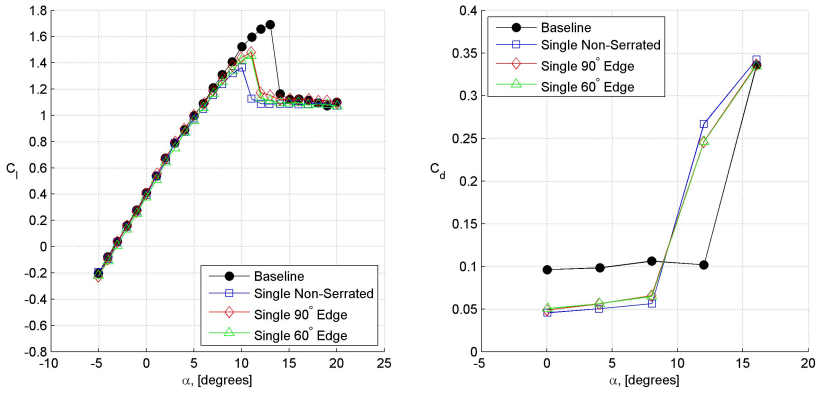

(a) (b)

Figure 4: Measured (a) lift and (b) drag curves for the FB-3500-1750 airfoil with a single splitter plate at $Re = 666{,}000$.

abstract. For all cases, the transition location is specified to match wind tunnel conditions.

The trailing edge devices investigated computationally include splitter plate lengths of 50%, 75%, 100%, and 150% t_{TE}. The 100% t_{TE} splitter plate was also investigated at two angles ($\pm 10°$) from center to determine the performance effects. Cavity and offset cavity studies were also conducted with lengths equal to 100% t_{TE}.

5 RESULTS

5.1 Wind Tunnel Results

The measured lift and drag characteristics for the single splitter plate configuration are presented in Fig. 4. The drag of the baseline airfoil was reduced by approximately 50% with the application of the splitter plate, with nominal variation for plate edge treatment. Figure 4(a) shows the application of a splitter plate to the FB-3500-1750 airfoil caused a moderate loss in maximum lift due to an ealier onset of stall compared to baseline, which was mitigated with the use of plate edge serrations.

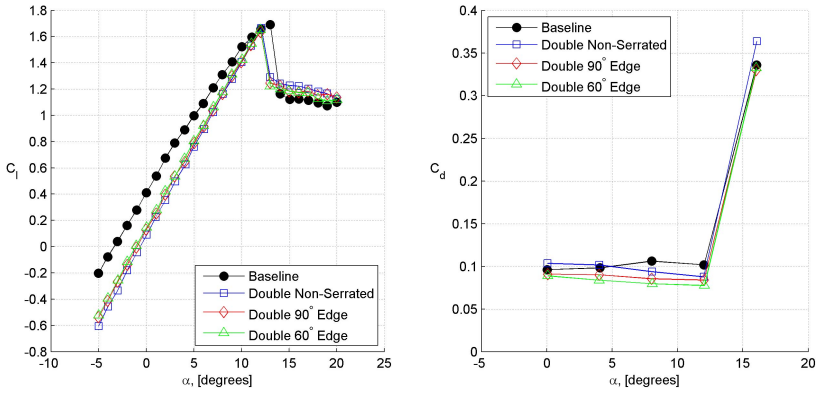

(a) (b)

Figure 5: Measured (a) lift and (b) drag curves for the FB-3500-1750 airfoil with a base cavity at $Re = 666{,}000$.

The base cavity also affected the lift and drag of the FB-3500-1750 airfoil, as shown in Fig. 5. In this case, the lift slope and the zero-lift angle of attack were increased compared to baseline, independent of edge treatment (Fig. 5(a)). The change in zero-lift angle of attack is

likely due to an effective reduction of airfoil camber, caused by the manner in which the cavity was applied to the airfoil, while the change in lift curve slope may be caused by an effective increase in airfoil chord. These effects were not present in the single splitter configuration, due to the massive flow separation over the surface of the plate. The airfoil with base cavity experienced up to 25% less drag than the baseline airfoil, as shown in Fig. 5(b), however, this drag reduction was dependent on both angle of attack and edge treatment.

5.2 Computational Results

A comparison of the computational and experimental results for the baseline airfoil and airfoil with 100% t_{TE} splitter is presented in Fig. 6. The calculated lift matches very well with experiment, except the stall angle of attack is overpredicted. This problem is much more acute for the baseline airfoil. Fig. 6(b) shows that the drag calculations are in excellent agreement with experiment for the splitter plate configuration, but agree poorly for the baseline airfoil. This trend may best be explained by the vortical wake structure for the baseline airfoil, and the lack thereof for the splitter plate configuration shown in Fig. 7. The Kármán vortex street is clearly evident for the baseline case, but is absent once the splitter plate is added. The unsteady vortical wake present in the baseline airfoil computations is probably qualitatively correct, but it is likely that the vortices' strengths were over-predicted due to the artificial restriction of the flow to two-dimensions.

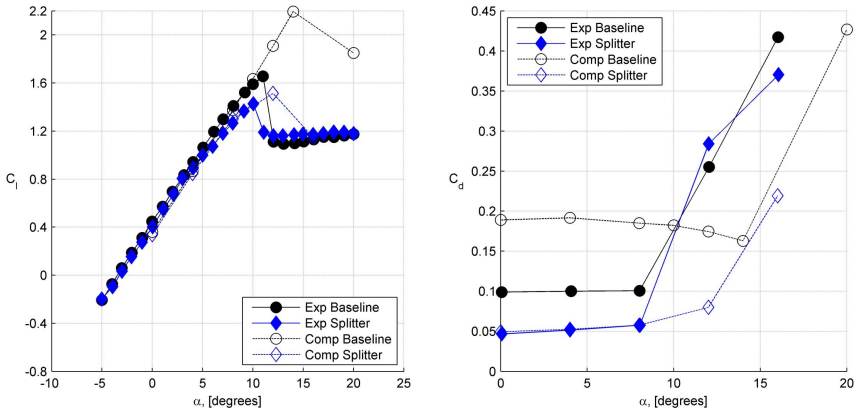

(a) (b)

Figure 6: Comparison of (a) lift and (b) drag for experiment and RANS computations, FB-3500-1750 airfoil at $Re = 666{,}000$.

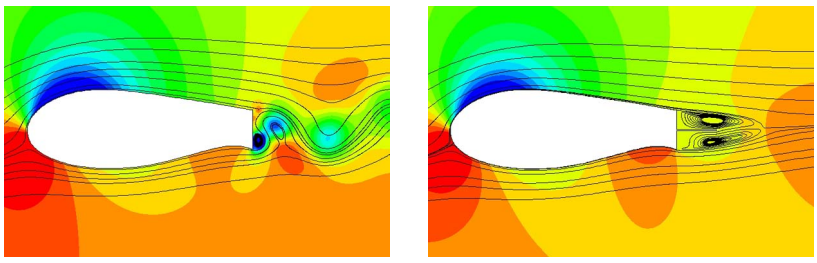

(a) (b)

Figure 7: Calculated pressure contours with instantaneous streamlines for the FB-3500-1750 airfoil at $Re = 666{,}000$ and 8° incidence with (a) no modifications, and (b) single splitter.

The computational results presented in Figs. 8 and 9 show the effects of splitter plate length and angle on lift and drag performance of the FB-3500-1750 airfoil. Splitter length has a dramatic affect on $C_{l_{max}}$ and, to a lesser extent, on lift curve slope. In the attached flow region, splitter length does not appear to affect the drag reduction, except for the 50% t_{TE}, which was less effective compared to the other lengths. Figure 9 indicates splitter plate angle does not influence drag reduction, but can impact the lift curve slope and maximum lift. Interestingly, the upward deflected plate ($+10°$) incremented the lift while the downward deflected plate ($-10°$) caused lift decrement, which is the opposite effect of a flap. This result requires further investigation.

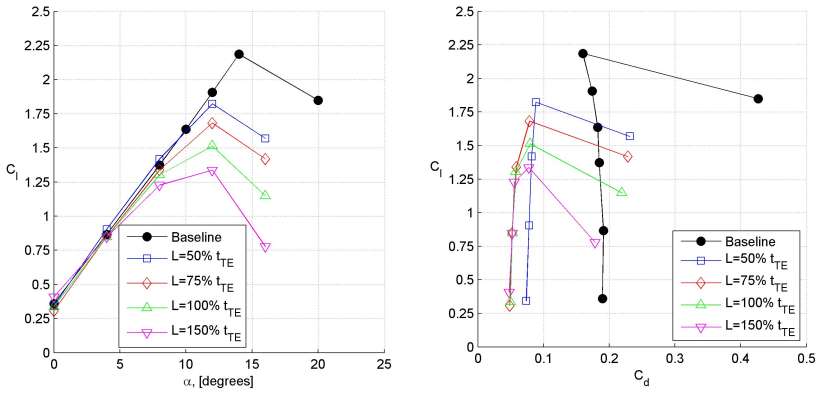

(a) (b)

Figure 8: The effect of splitter plate length on computational (a) lift and (b) drag polars for the FB-3500-1750 airfoil at $Re = 666{,}000$.

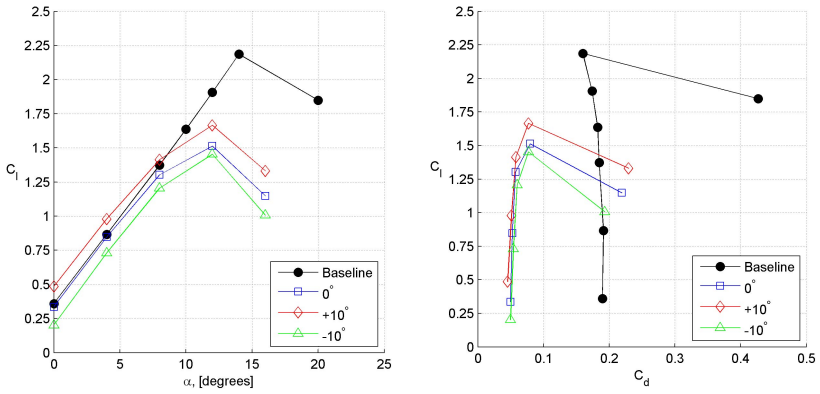

(a) (b)

Figure 9: The effect of splitter plate angle on computational (a) lift and (b) drag polars for the FB-3500-1750 airfoil at $Re = 666{,}000$. Angle defined + for upward deflection. L = 100% t_{TE}.

REFERENCES

[1] Van Rooij, R. and Timmer, W., "Roughness Sensitivity Considerations for Thick Rotor Blade Airfoils," *Journal of Solar Energy Engineering*, Vol. 125, No. 4, November 2003, pp. 468–478.

[2] Baker, J., Mayda, E., and van Dam, C., "Experimental Analysis of Thick Blunt Trailing-Edge Wind Turbine Airfoils," *Journal of Solar Energy Engineering*, Vol. 128, No. 4, 2006, pp. 422–431.

[3] Winnemöller, T. and van Dam, C., "Design and Numerical Optimization of Thick Airfoils Including Blunt Trailing Edges," *Journal of Aircraft*, Vol. 44, No. 1, 2007, pp. 232–240.

[4] Standish, K. J. and van Dam, C., "Aerodynamic Analysis of Blunt Trailing Edge Airfoils," *Journal of Solar Energy Engineering*, Vol. 125, No. 4, November 2003, pp. 479–487.

[5] Hoerner, S., "Base Drag and Thick Trailing Edges," *Journal of the Aeronautical Sciences*, Vol. 17, No. 10, 1950, pp. 622–628.

[6] Smith, H. A. and Schaefer, R. F., "Aerodynamic Characteristics at Reynolds Numbers of 3.0×10^6 and 6.0×10^6 of Three Airfoil Sections Formed by Cutting Off Various Amounts from the Rear Portion of the NACA 0012 Airfoil Section," Tech. Rep. TN-2074, NACA, 1950.

[7] Law, S. P. and Gregorek, G. M., "Wind Tunnel Evaluation of a Truncated NACA 64-621 Airfoil for Wind Turbine Applications," Tech. Rep. CR-180803, NASA, July 1987.

[8] Roshko, A., "On the Wake and Drag of Bluff Bodies," *Journal of Aeronautical Sciences*, Vol. 22, 1955, pp. 124–132.

[9] Bearman, P., "Effect of Base Bleed on Flow Behind Two-Dimensional Model with Blunt Trailing Edge," *Aeronautical Quarterly*, Vol. 18, No. 3, 1967, pp. 207–224.

[10] Tanner, M., "A Method for Reducing the Base Drag of Wings with Blunt Trailing Edge," *Aeronautical Quarterly*, Vol. 23, No. 1, February 1972, pp. 15–23.

[11] Molezzi, M. J. and Dutton, J. C., "Study of Subsonic Base Cavity Flowfield Structure Using Particle Image Velocimetry," *AIAA Journal*, Vol. 33, No. 2, February 1995, pp. 201–209.

[12] Chng, T. L. and Tsai, H. M., "Effects of Spanwise Geometric Disturbances on a Bluff Body Wake," 3^{rd} *AIAA Flow Control Conference*, AIAA-2006-3338, San Francisco, CA, June 5-8 2006.

[13] Tanner, M., "Reduction of Base Drag," *Progress in Aerospace Sciences*, Vol. 16, No. 4, 1975, pp. 369–384.

[14] TPI Composites, Inc., "Innovative Design Approaches for Large Wind Turbine Blades – Final Report," Tech. Rep. SAND2004-0074, Sandia National Laboratories, March 2004.

[15] Aerolab, *Operating Handbook for the UC Davis Low Turbulence Tunnel*, Laurel, MD, 1996.

[16] Buning, P., Jespersen, D., Pulliam, T., Klopfer, G., Chan, W., Slotnick, J., Krist, S., and Renze, K., *OVERFLOW Users Manual 1.8aa*, NASA Langley Research Center, Hampton, Virginia, April 2003.

[17] Chan, W., Rogers, S., Nash, S., Buning, P., and Meakin, R., *Users Manual for Chimera Grid Tools, Version 1.9*, NASA Ames Research Center, October 2004.

[18] Menter, F. R., "Performance of Popular Turbulence Models for Attached and Separated Adverse Pressure Gradient Flows," *AIAA Journal*, Vol. 30, No. 8, 1992, pp. 2066–2072.

[19] Menter, F. R., "Two-Equation Eddy-Viscosity Turbulence Models for Engineering Applications," *AIAA Journal*, Vol. 32, No. 8, 1994, pp. 1598–1605.

[20] Kral, L., "Recent Experience with Different Turbulence Models Applied to the Calculation of Flow Over Aircraft Components," *Progress in Aerospace Sciences*, Vol. 34, No. 7-8, November 1998, pp. 481–541.